Journal of Hydrology 378 (2009) 161–167

Contents lists available at ScienceDirect

Journal of Hydrology

journal homepage: www.elsevier.com/locate/jhydrol

Estimating the snow water equivalent from snow depth measurements in the Swiss Alps

T. Jonas *, C. Marty, J. Magnusson

WSL Institute for Snow and Avalanche Research SLF, Flüelastr. 11, 7260 Davos, Switzerland

ARTICLE INFO

Article history:
Received 1 April 2009
Received in revised form 10 August 2009
Accepted 5 September 2009

This manuscript was handled by K. Georgakakos, Editor-in-Chief

Keywords:
Snow hydrology
Mountain water resources
Seasonal snow
Spatiotemporal variability
Switzerland

SUMMARY

The snow water equivalent (*SWE*) characterizes the hydrological significance of snow cover. However, measuring *SWE* is time-consuming, thus alternative methods of determining *SWE* may be useful. *SWE* can be calculated from snow depth if the bulk snow density is known. Thus, a reliable estimation method of snow densities could (a) potentially save a lot of effort by, at least partly, sampling snow depth instead of *SWE*, and would (b) allow snow hydrological evaluations, when only snow depth data are available. To generate a useful parameterization of the bulk density a large dataset was analyzed covering snow densities and depths measured biweekly over five decades at 37 sites throughout the Swiss Alps. Four factors were identified to affect the bulk snow density: season, snow depth, site altitude, and site location. These factors constitute a convenient set of input variables for a snow density model developed in this study. The accuracy of estimating *SWE* using our model is shown to be equivalent to the variability of repeated *SWE* measurements at one site. The technique may therefore allow a more efficient but indirect sampling of the *SWE* without necessarily affecting the data quality.

Introduction

Under a changing climate, mountain water resources become increasingly important. In mountainous catchments snowmelt typically constitutes a significant part of the total runoff (Barnett et al., 2005; Hock et al., 2006). Therefore, keeping track of the spatial and temporal distribution of snow is vital for monitoring mountain water resources and predicting subsequent runoff. For hydrological applications, we need to characterize the snow cover by its snow water equivalent (*SWE*).

Measuring *SWE* requires substantially more effort than it does to sample snow depth. However, as will be shown later, *SWE* is strongly correlated to the snow depth (*HS*). This correlation could potentially be used to estimate *SWE* from *HS*. Thus, studies have suggested enhancing sampling efficiency by substituting a significant part of the time-consuming *SWE* measurements by simple *HS* measurements (Elder et al., 1998; Rovansek et al., 1993). However, here we shall try to completely abandon *SWE* measurements and assess that parameter from *HS* sampling alone.

The ratio *SWE*/*HS* at a single point is referred to as bulk snow density (ρb),

$$SWE = HS \cdot \rho b \quad (1)$$

Thus, estimating *SWE* from *HS* is the same task as estimating ρb. Sturm et al. (2009) recently came up with a ρb model with respect to snow depth and snow class (Sturm et al., 1995). Their study was based on over 25,000 *SWE*–*HS*–ρb records measured in several countries over several decades. Here, we specifically address a regional parameterization of ρb for seasonal snow in the Swiss Alps that emphasizes the temporal evolution of ρb.

Given the complex topography and frequent snow redistribution processes in alpine environments, *SWE* typically displays a considerable spatial variability even within a given sample site (Bray, 1973; Liston and Sturm, 2002). Hence, to establish a *SWE* value representative of such a site, several *SWE* measurements would be necessary (Watson et al., 2006). However, with special regard to catchment-scale water resource monitoring, such an effort seems unrealistic and we shall regard the expenditure of one *SWE* measurement per site as a practical limit. Here, we hypothesize that a few *HS* measurements converted to *SWE* using the proposed ρb model characterize a site as good as a single *SWE* measurement but at less effort. This would allow putting the freed resources in sampling at more sites. Moreover, the approach would also include the possibility to convert historic *HS* data into *SWE* in the absence of other information than sampling date and location.

Snow data

The WSL Institute for Snow and Avalanche research SLF runs an extensive snow monitoring network in the Alps (Fig. 1), which was

* Corresponding author. Tel.: +41 81 417 0259; fax: +41 81 417 0110.
E-mail addresses: jonas@slf.ch (T. Jonas), marty@slf.ch (C. Marty), magnusson@slf.ch (J. Magnusson).

0022-1694/$ - see front matter © 2009 Elsevier B.V. All rights reserved.
doi:10.1016/j.jhydrol.2009.09.021

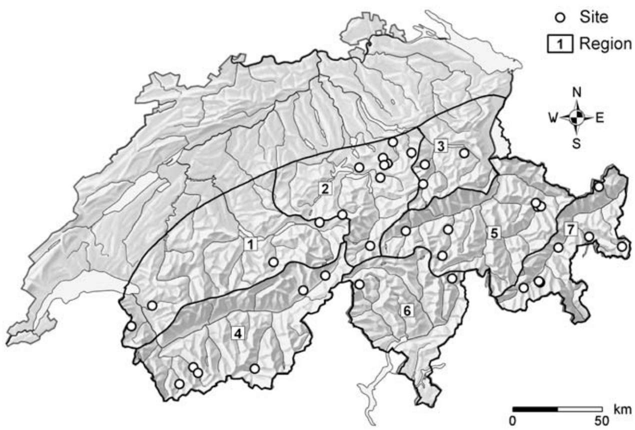

Fig. 1. Snow station sites and regions in Switzerland.

initiated about six decades ago by the Swiss Federal Institute of Technology (ETH). *SWE* is sampled biweekly (i.e. twice a month) by professional staff, all trained to the same standards. Snow cores are taken using aluminum cylinders with a cross-sectional area of 70 cm^2. On principle, a pit is dug to ensure that no snow is lost when extracting the core from the snow cover (i.e. the core is taken outside the pit and extracted laterally into the pit). Moreover, this procedure ensures most accurate simultaneous *HS* measures on the same spot. The measuring sites are typically flat and open. Note that although ρb is calculated from *HS* and *SWE* and thus not measured directly, *HS*/*SWE* will be referred to as the observed ρb in the following.

From our database we selected only records from sites that provided continuous long-term datasets of at least 20 years (on average 35 years) and followed the regular sampling scheme. This selection procedure resulted in 11,147 *SWE*-*HS*-ρb data records from 48 winters (1960–2008) and 37 stations throughout the Swiss Alps (Fig. 1). The sites cover an altitudinal range of 860–2690 m asl. However, note that for historical reasons the majority of the sites are located below 2000 m asl. Automatic plausibility checks consisted of testing the data records to satisfy Eq. (1). Furthermore data with ρb below 50 and above 600 kg/m^3, respectively, were discarded.

The SLF distinguishes between seven snow-climate regions in the Swiss Alps (Fig. 1). They reflect typical regional patterns in snow cover climatology. As the region assignment constitutes a potential ρb model input, all data have been attributed to their respective region via site location.

The systematic snow samples resulted in typical distributions of *SWE*, *HS*, and ρb values: While the ρb data are approximately normally distributed, *SWE* and *HS* data clearly exhibit a log-normal distribution (Fig. 2). The evolution of the snow cover varies considerably from year to year and from site to site (data not shown). Accumulation and melting of snow follows amongst other factors the precipitation and temperature patterns (Elder et al., 1991; Laternser and Schneebeli, 2003).

Relationship between water equivalent, density, and depth of snow

Snow depth, bulk density and water equivalent are related to one another according to Eq. (1). The pair-wise correlations between these three snow cover properties are presented in Fig. 3. As expected, *SWE* and *HS* display a strong correlation, which seems approximately linear (Fig. 3a). However, on closer examination the best-fit line is slightly curved upward. This statement is identical to the finding that the mean ρb increases with *HS* (Fig. 3b; Lundberg et al., 2006; Marchand and Killingtveit, 2004; Pomeroy and Gray, 1995). ρb was fitted to *HS* using a power curve (Fig. 3b),

$$\rho b = 60.1 \cdot HS^{0.89} + 237 \tag{2}$$

Multiplying this equation with *HS* results in a corresponding fit for *SWE* to *HS* (Fig. 3a),

$$SWE = (60.1 \cdot HS^{0.89} + 237) \cdot HS \tag{3}$$

where in both Eqs. (2) and (3) *SWE* is in kg/m^2, *HS* in m, and ρb in kg/m^3.

The variance of the data shown is clearly non-uniform (i.e. heteroscedastic). In particular, a meaningful density model needs to cope with the pronounced variability of ρb at low snow depths. A reason for this behavior is that a shallow snow cover can range from low-density new snow in autumn to high-density slush in spring. We may therefore expect a seasonal evolution of ρb.

A direct plot of ρb versus time shows that the bulk density gradually increases over the course of the winter season (Fig. 4a). This effect has been reported by many previous studies (Anderton et al., 2004; Elder et al., 1991; Mizukami and Perica, 2008; Rohrer et al., 1994; Sturm and Holmgren, 1998) and corresponds to the increasing compaction of snow due initially to settling and later to snow cover ripening. A relevant implication of the seasonal evolution of ρb is the distinct shape of the *SWE*-*HS* trajectories (Fig. 4b). Comparing these trajectories with the data shown in Fig. 3a, reveals that accounting for the seasonal evolution of ρb provides a promising tool to enhance *SWE* estimations from *HS*.

Besides time of the year and *HS* there are many other factors that may potentially enhance the accuracy of ρb estimations. However, to stay in line with the purpose of this paper we shall concentrate on factors that are accessible without substantial extra effort. One of these easy-to-gather factors is the site location. The effect of location was tested by considering region (Fig. 1) and altitude.

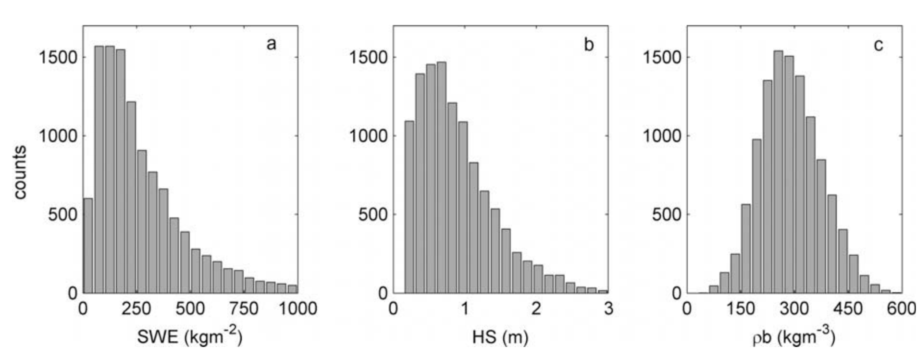

Fig. 2. Distribution of *SWE*, *HS*, and ρb data sampled biweekly at 37 sites throughout the Swiss Alps over five decades (n = 11,147).

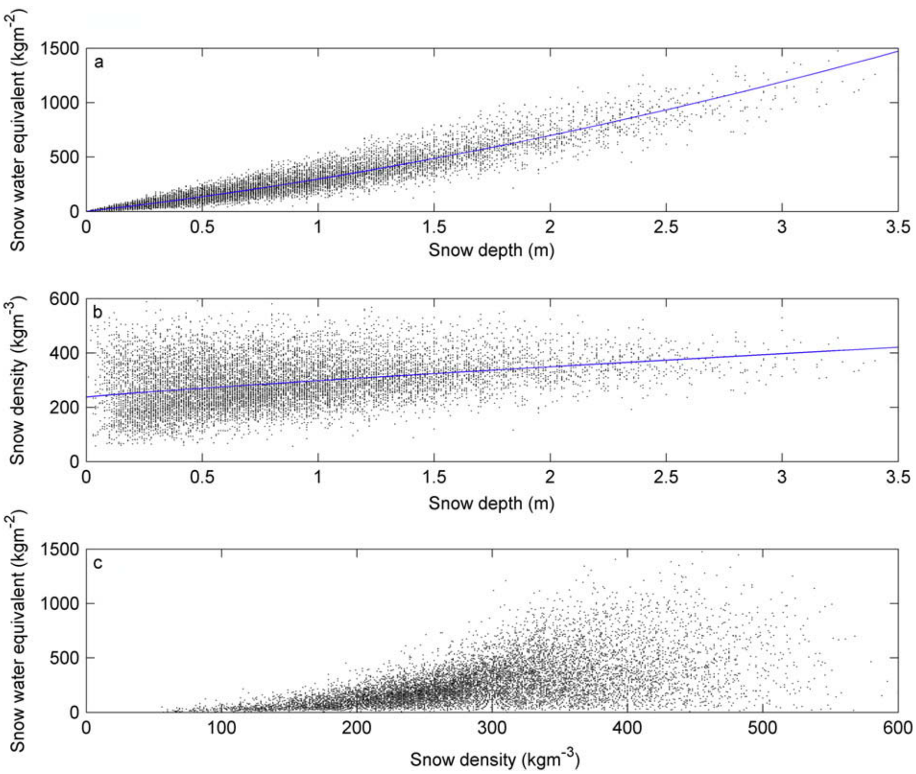

Fig. 3. The relationship between *SWE*, ρb, and *HS*. The best-fit lines are specified in Eqs. (2) and (3).

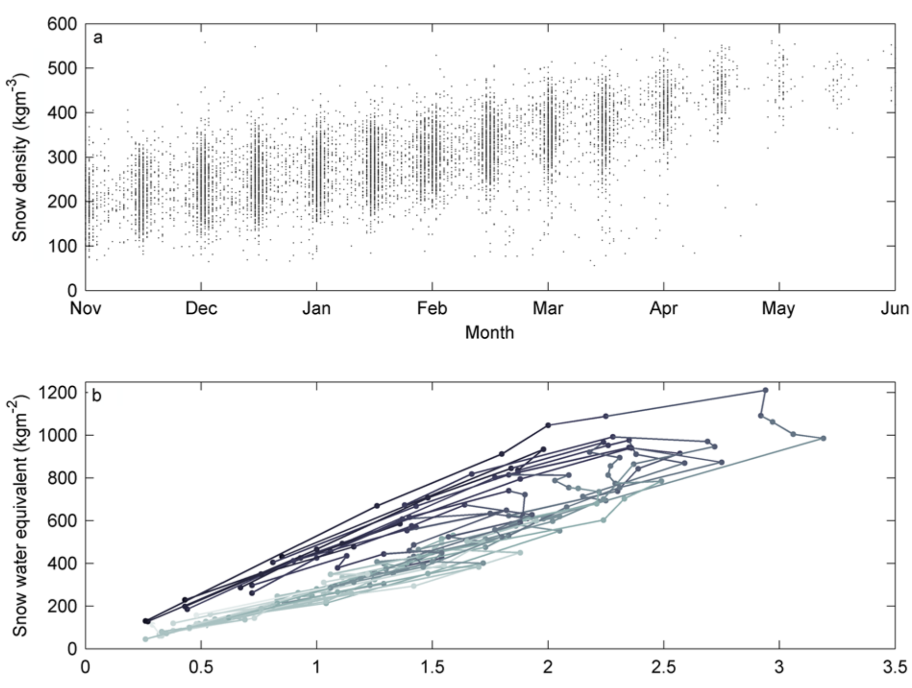

Fig. 4. The effect of season on bulk snow density. Panel b displays typical seasonal *SWE–HS* trajectories (exemplary data from station Weissfluhjoch at 2560 m asl.). Light to dark gray colors denote months November–June.

Not surprisingly, there were considerable differences between regions with regards to mean snow depths (not shown). These findings can be linked to the precipitation and temperature patterns in Switzerland (Laternser and Schneebeli, 2003). However, mean bulk densities differed only slightly between regions. Expectedly, regions #4, #5, and #7 displayed the lowest mean ρb, as they are dominated by a dry, inner-alpine climate.

The altitude has only a minor direct effect on the average ρb (Fig. 5a). This result may appear rather counter-intuitive, as higher snow depths at higher sites should entail increased mean ρb.

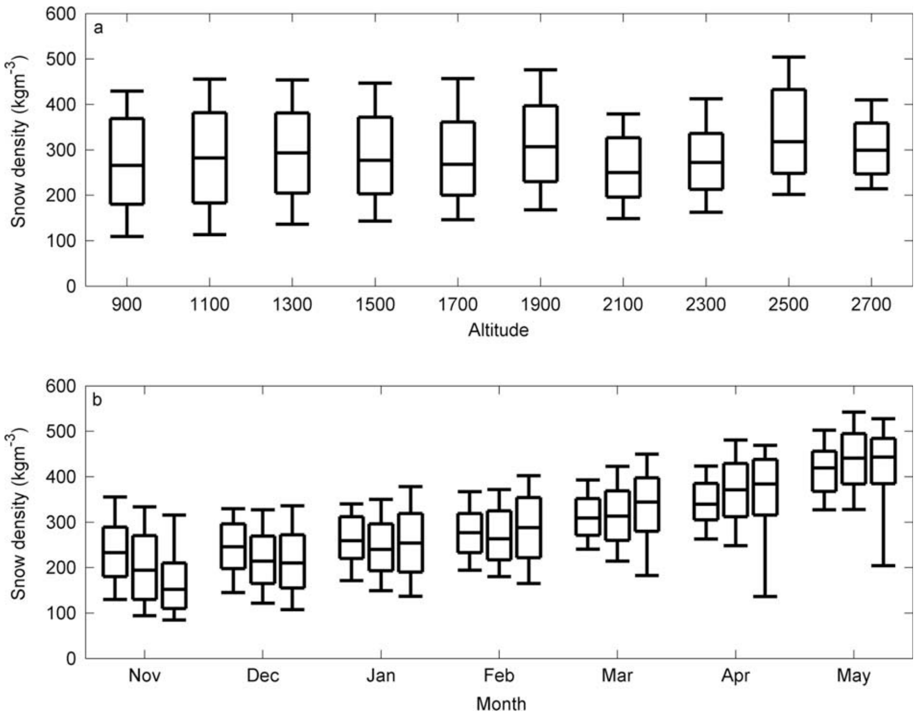

Fig. 5. The effect of altitude on bulk snow density. Distribution of ρb data split up into altitudinal subsets, seasonal subsets, respectively. Box plots display the median value ±1 standard deviation, the whiskers denote median ±2 standard deviations. Data in panel b are staggered with respect to site altitude (left: $\geqslant$2000 m; center: $\geqslant$1400 m and <2000 m; right: <1400 m).

Warmer temperatures at lower altitudes may, however, induce a compensating effect (cf. Onuchin and Burenina, 1996). Nevertheless, altitude remains an interesting variable with respect to the ρb model. The interaction between the factors altitude and season reveals an indirect effect on ρb (Fig. 5b; see also Mizukami and Perica, 2008). The data show that in early winter ρb increases with altitude, which is likely related to the fact that at this time of the year only higher altitudes feature considerable snow depths. However, in late winter the opposite is the case, and ρb decreases with altitude, because the melt-out progresses faster at lower altitudes.

Further, sun exposure was tested for its direct or indirect effects on ρb. All the sites were manually classified as sun-exposed, normal, or shady. However, we did not find any considerable difference between these three classes with respect to ρb.

Parameterization of the bulk snow density

The main purpose of the ρb model is to facilitate *SWE* monitoring on the catchment scale. It should allow converting measured *HS* values into *SWE*. However, to be an efficient technique the model should only require input data that can be recorded during a *HS* survey with little additional effort. Clearly, for some applications factors such as local insolation charts or previous meteorological conditions are too laborious to handle or unavailable. Moreover, the model needs to be applicable at other sites and to other times than those covered by our dataset, i.e. year and site identifier are not appropriate input factors either.

Thus far, four factors could be identified with a notable effect on ρb: (1) season, (2) *HS*, (3) site altitude, and (4) region. Gathering these factors only requires recording location and date when sampling *HS*. Therefore, they are appropriate input factors for the ρb model.

Given the complex non-linear and interacting relationship between the four input factors and ρb, we opted for a model combining the flexibility of look-up tables with the efficiency of data fitting. In a first step the dataset was split up into three times 12 subsets (cf. Fig. 5b) according to three altitude range classes ($\geqslant$2000 m, $\geqslant$1400 m and <2000 m, <1400 m) and 12 seasonal classes (months), respectively. Then, ρb was fitted to *HS* data for each data subset separately using linear regression. Non-linear regression did not enhance the fit; neither did fitting to log-transformed *HS* data (cf. Fig. 2b). For simplicity, we retained the linear model approach. The procedure resulted in two regression coefficients per subset (Table 1). The table allows an estimation of preliminary ρb values from *HS* data

$$\rho b_{prel.} = a \cdot HS_{obs.} + b, \tag{4}$$

where $[b, a]$ are to be selected from Table 1 according to site altitude and recording date.

The preliminary ρb model accounts for three out of four designated input factors, with region not yet included. Therefore, the full dataset has been split up in seven subsets according to the regions defined in Fig. 1. Per subset the model residuals $\rho b_{prel.} - \rho b_{obs.}$ were calculated and averaged yielding region-specific density offsets (Table 2). These offset values may be used to enhance ρb estimations in Switzerland according to

$$\rho b_{mod.} = a \cdot HS_{obs.} + b + \text{offset}_{reg.}, \tag{5}$$

where $\text{offset}_{reg.}$ is to be selected from Table 2 according to region. Finally, *SWE* can be deduced as

$$SWE_{mod.} = HS_{obs.} \cdot \rho b_{mod.} \tag{6}$$

The type of model may appear simplistic. However, the combination of look-up tables with regression analysis allows reflecting the complex and non-linear interactions between the four terms with relevant effects on ρb, while at the same time the application remains user friendly.

Table 1
Look-up table for regression coefficients [b, a]. The bulk snow density can be calculated from snow depth according to Eq. (4). (n, R) denote the number of data records used for the regressions and the correlation coefficients in %, respectively.

	Altitudes (asl.) ⩾2000 m [b, a]; (n, R)	Altitudes (asl.) ⩾1400 m and <2000 m [b, a]; (n, R)	Altitudes (asl.) <1400 m [b, a]; (n, R)
October	na.[a]	na.	na.
November	[206, 47]; (116, 27)	[183, 35]; (198, 16)	[149, 37]; (141, 14)
December	[203, 52]; (237, 45)	[190, 47]; (864, 31)	[201, 26]; (625, 13)
January	[206, 52]; (234, 58)	[208, 47]; (1145, 35)	[235, 31]; (866, 18)
February	[217, 46]; (235, 53)	[218, 52]; (1198, 48)	[279, 9]; (916, 6)
March	[272, 26]; (247, 38)	[281, 31]; (1218, 29)	[333, 3]; (826, 2)
April	[331, 9]; (214, 13)	[354, 15]; (828, 14)	[347, 25]; (451, 17)
May	[378, 21]; (124, 22)	[409, 29]; (273, 26)	[413, 19]; (88, 11)
June	[452, 8]; (81, 11)	na.	na.
July	[470, 15]; (22, 20)	na.	na.

[a] Too little data available to establish a regression model.

Table 2
Look-up table for region-specific offsets, cf. Eq. (5). n denotes the number of data records available per region.

Region	1	2	3	4	5	6	7
Offset (kg/m^3)	+7.6	+11.7	+11.8	−1.1	−0.3	+12.1	−14.7
n	893	2989	1171	1535	2330	535	1694

Model test

The model was evaluated in several ways: using in-sample tests, analyzing the model's transferability to independent data, and by testing the effect of model simplifications. As a first test of the model performance, $\rho b_{mod.}$ and $SWE_{mod.}$ were calculated from the observed HS data and compared to $\rho b_{obs.}$ and $SWE_{obs.}$, respectively (Fig. 6). While the bulk of the estimated ρb data (±1 standard deviation) matches the observed data within a range of ±45 kg/m^3, the scatter of the residuals is considerable (Fig. 6a). However, this finding is not astonishing, as the model was not designed to account for previous meteorological conditions that governs the evolution of the snowpack sampled (Meloysund et al., 2007; Onuchin and Burenina, 1996; Sturm and Holmgren, 1998). Especially in lower regions, the meteorological history is decisive (Rohrer et al., 1994). Accordingly, specific error bounds for a data subset from lower sites display a greater model uncertainty than respective results for sites at higher altitudes. As for the SWE, estimated values compare well with observed data (Fig. 6b). The bulk of the estimates (±1 standard deviation) are on average within 16% of the observed value, with a tendency for better results at high SWE, worse results at low SWE respectively. The model performance with respect to SWE yields much better results than the respective comparison for ρb, which corresponds to the observation that most of the variability in SWE is explained by the variability of HS (Fig. 3a; Pomeroy and Gray, 1995).

To gain more insight into the model performance, we identified those 10% of the $\rho b_{mod.}$ data with the highest bias relative to $\rho b_{obs.}$, termed as $\rho b_{w10\%}$ in the following. It was then tested whether data from specific months, altitudes, or snow depths were significantly

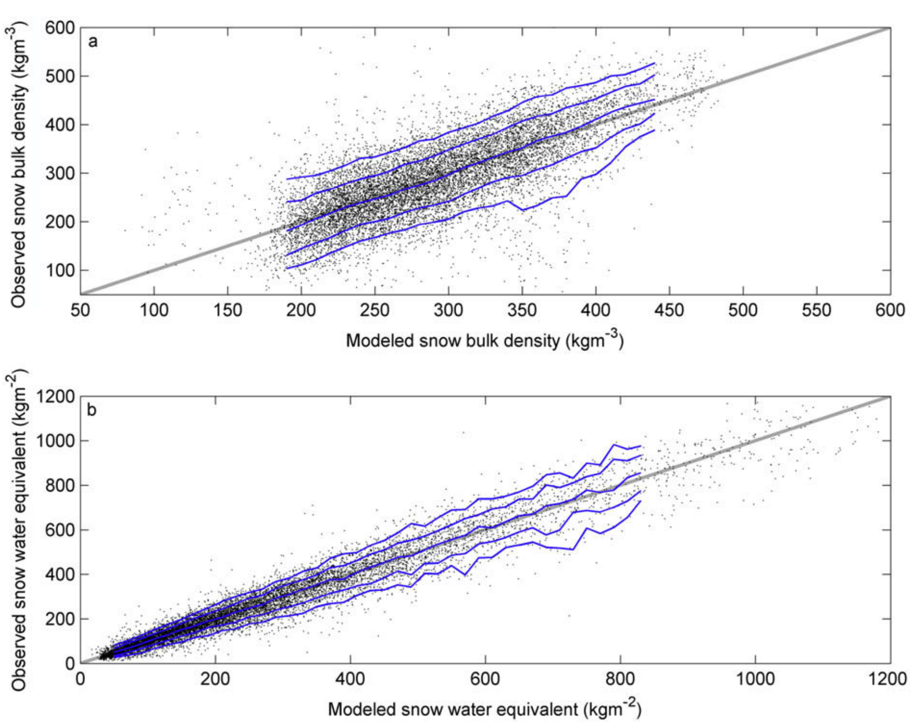

Fig. 6. Observed versus modeled bulk snow density and snow water equivalent, respectively. The solid blue lines indicate gliding prediction bounds corresponding to median, ±1 standard deviation (inner bounds), and ±2 standard deviations (outer bounds), respectively. (For interpretation of the references to colours in this figure legend, the reader is referred to the web version of this paper).

Table 3
Model test: *RMSE* of $SWE_{mod.} - SWE_{obs.}$ using different validation datasets (V1–V3) and alternative models (A1–A5). Validation datasets for model configurations V1–V3 are described in the section Model test. Alternative models A1–A5 were tested against the full dataset, where the table specifies (×), which of the four available effects were accounted for.

Model	Month	Altitude	*HS*	Region	*RMSE*
V1	×	×	×	×	50.9
V2	×	×	×	×	51.3
V3	×	×	×	×	53.2
A1	×		×		53.3
A2	×	×			58.1
A3		×	×		73.0
A4[a]			×		72.3
A5[b]					88.7

[a] $\rho b_{mod.}$ according to Eq. (2).
[b] Model uses a constant $\rho b_{mod.}$ = median ($\rho b_{obs.}$).

overrepresented in $\rho b_{w10\%}$. With respect to season, the analysis revealed that only ρb predictions for November were overrepresented in the subsample with the highest bias (20% of all November data were contained in $\rho b_{w10\%}$). November had the highest variability in observed ρb with snow types ranging from light new snow to melting ephemeral snow. Similarly, the lowest altitudes displayed higher bias of $\rho b_{mod.}$ (22% of all data sampled below 1000 m asl. were contained in $\rho b_{w10\%}$). While at higher altitudes the snow season typically displays a clearly defined accumulation period followed by the ablation period, at lower altitudes melting may occur episodically throughout the entire snow season, which causes greater variability in observed ρb. Finally, shallow snowpacks were overrepresented in the subsample with the highest bias of $\rho b_{mod.}$ (23% of all data with *HS* < 0.25 m, were contained in $\rho b_{w10\%}$). This effect could be attributed to the lowest values of $\rho b_{obs.}$, which invariably occurred at low snow depths, where these extreme values seem difficult to capture by a stochastic approach. Summarizing and not astonishing, the model displays notable difficulties to predict $\rho b_{mod.}$ for low-altitude, early-season, and shallow snowpacks. These circumstances favor the occurrence of ephemeral snow, the density of which is hard to predict without accounting for previous meteorological conditions.

To test the transferability of the model to independent data, $\rho b_{mod.}$ and $SWE_{mod.}$ from observed *HS* data were compared to $\rho b_{obs.}$ and $SWE_{obs.}$ using three configurations of model calibration data versus model validation data (Table 3): first, all data used to calibrate the final model above were also used for validation (V1). Second, the model was cross-validated using a tenfold 90%/10% data splitting (V2). Therefore, random 10% of the data were excluded from the data pool for model calibration and subsequently used as independent validation data. This step was repeated further nine times, where as each dataset could only once be drawn for the cross-validation. And third, the model was tested against 2188 datasets (V3) from snow stations that were excluded from the final model calibration when their records did not meet the required length of at least 20 years (cf. Snow data section). Note that a random draw procedure was applied to ensure the validation dataset to feature the same snow depth distribution as shown in Fig. 2. Additionally, the effect of simplifications of the final model on its performance was tested (Table 3). Model simplifications A1–A5 were realized by neglecting the effects of season, site altitude, snow depth, and site location on $\rho b_{mod.}$ separately or combinedly.

The model's *RMSE* using the calibration data for validation (Table 3, V1) is used as the benchmark performance. The cross-validation (V2) displays a practically identical performance, while the validation with alternative data (V3) results in a minor reduction of the model performance. The model seems thus quite robust with respect to transferability to independent data. Remarkably, also the alternative model A1 achieves a *RMSE* similar to the benchmark performance. Obviously the effects of site altitude and location (in Switzerland) are minor compared to the effects of season and snow depth on ρb. This finding suggests that the model presented in this study may also be applicable to snow depth data from areas outside the Swiss Alps, provided similar climatologic conditions. Even an extrapolation to climate predicted for the near future may be appropriate, since expected snow cover changes in the Alps seem to resemble snow regimes existing today but at lower altitudes (Bavay et al., 2009; Magnusson et al., 2009). The validation of alternative models A2–A4 reveals that neglecting either the effect of snow depth or the effect of season on ρb significantly increases the model bias. Of these two effects the seasonal variation in ρb seems clearly more important for incorporation in the model. The same conclusion can also be drawn when comparing the magnitude of both effects in the respective univariate plots (Figs. 3b and 4a).

Utility of the model

It was initially hypothesized that a few *HS* measurements converted to *SWE* using the ρb model characterize a site as good as a single *SWE* measurement but at less effort. To test the hypothesis, the model residuals are compared to the variability of repeated *SWE* measurements at one site. There is surprisingly little data published on the within-site variability of both, *SWE* and ρb. More-

Table 4
Within-site variability of bulk snow density and snow water equivalent according to literature and field experiments. A description of the studies (1)–(4) can be found in the papers referenced below. The Swiss experiments were conducted nearby Davos on flat and open field sites between 1560 and 2200 m asl. using the same measurement techniques as described in the section Snow data.

Citation	(1)	(2)	(3)	(4)	(5)	(5)	(5)
Country	USA	Canada	Canada	Canada	Switzerland	Switzerland	Switzerland
Season	Mid winter	Diff. times	February	Pre-melt	Early winter	Mid winter	Late winter
Approx. *HS*	70 cm	55 cm	55 cm	–	46 cm	152 cm	51 cm
Sampling spacing	10 m	1 m	Random	5 m	5/10 m	5/10 m	5 m
Sampling design	100 m lines	8 × 8 m grid	50 m radius	100 × 100 m grid	25 × 25 m grid	25 × 25 m grid	25 × 25 m grid
Number of samples	1240	108	322	437	18	18	36
HS compensation (6)	Yes	Yes	No	No	No	No	No
Variability ρb (7)	23%	21%	11–20%	–	8%	7%	15%
Variability *SWE* (7)	23%	21%	23–27%	36–80%	18%	13%	30%

(1) Sturm and Liston, (2003).
(2) Bray, (1973).
(3) Kershaw and McCulloch, 2007).
(4) Janowicz et al., (2003).
(5) Own experiment.
(6) Data was corrected with reference to site-averaged HS_{mean}, i.e.: $SWE_{corr.} = SWE_i - (HS_i - HS_{mean}) \cdot \rho b_{mean}$; $\rho b_{corr.} = SWE_{corr.}/HS_{mean}$.
(7) One standard deviation/mean.

over, it is arguable whether respective results from different studies can be compared because of different length scales, different snow regimes, and sampling techniques with different accuracies involved. Nevertheless, Table 4 shall give a rough overview on the within-site variability of *SWE* and ρb.

The data compilation in Table 4, suggests that 10–20% is a typical range for the within-site variability of repeated ρb measurements. Superposed variations in *HS* seem to augment the within-site variability of *SWE* where a typical range may be conservatively given as 15–25%. Comparing this number with the variance of the model residuals (16%, Model test section), we may accept the initial hypothesis suggesting that the ρb model in combination with few *HS* measurements characterizes a site as well as a single *SWE* measurement.

Note that the model may not be suitable to convert time series of *HS* into *SWE* at daily resolution or higher. Transient phenomena such as the settling of recently fallen fresh snow cannot be comprehended by the model. Converted time series may therefore feature an incorrect fine structure in the temporal course of *SWE*.

Conclusions

This study attempts to enhance estimations of the snow water equivalent from snow depth observations on the condition that no additional measurements shall be required. Given Eq. (1), this task corresponds to finding a feasible parameterization of the bulk snow density. We therefore investigated how the bulk snow density is affected by snow depth and other factors that could be derived from recording date and location. The analysis is based on 11,147 records of snow densities and depths measured over five decades at 37 sites throughout the Swiss Alps.

Four factors were identified to feature a relevant effect on bulk snow density, which are (ordered by relevance): season, snow depth, site altitude, and snow-climate region. These factors were consequently used as input for a new bulk snow density model primarily applicable to seasonal snow in the Swiss Alps. However, the minor importance of regional effects suggests that the model may also be applicable in other regions with similar snow climatologic conditions. The model combines look-up tables with regression analysis and is very easy to use.

Applying the model to different datasets of combined snow depth and water equivalent measurements enabled comparing estimated snow densities with corresponding verification data. The model uncertainty was found to be of the same order of magnitude as the variability of repeated measurements at one site. We hence conclude that modeled bulk densities and snow water equivalents can represent a given site as well as respective single-point measurements. Depending on the application, this approach may consequently allow substituting time-consuming snow water equivalent measurements by a few snow depth samples.

Acknowledgements

We wish to thank all known and unknown colleagues that were involved in collecting the snow data over five decades, without whom this study would not have been possible. Data from three out of 37 snow stations were provided by Mario Rohrer. We also thank Manfred Stähli, Ethan M. Greene, Martin Schneebeli, Noah Molotch, and Keith Musselman for their helpful comments on this manuscript.

References

Anderton, S.P., White, S.M., Alvera, B., 2004. Evaluation of spatial variability in snow water equivalent for a high mountain catchment. Hydrological Processes 18 (3), 435–453.

Barnett, T.P., Adam, J.C., Lettenmaier, D.P., 2005. Potential impacts of a warming climate on water availability in snow-dominated regions. Nature 438 (7066), 303–309.

Bavay, M., Lehning, M., Jonas, T., Lowe, H., 2009. Simulations of future snow cover and discharge in Alpine headwater catchments. Hydrological Processes 23 (1), 95–108.

Bray, D.I., 1973. A report on the variability of snow water equivalent measurements at a site. In: In: Proceedings of the 30th Eastern Snow Conference, pp. 20–31.

Elder, K., Dozier, J., Michaelsen, J., 1991. Snow accumulation and distribution in an Alpine watershed. Water Resources Research 27 (7), 1541–1552.

Elder, K., Rosenthal, W., Davis, R.E., 1998. Estimating the spatial distribution of snow water equivalence in a montane watershed. Hydrological Processes 12 (10–11), 1793–1808.

Hock, R., Rees, G., Williams, M.W., Ramirez, E., 2006. Preface – contribution from glaciers and snow cover to runoff from mountains in different climates. Hydrological Processes 20 (10), 2089–2090 (special issue).

Janowicz, J.R., Gray, D.M., Pomeroy, J.W., 2003. Spatial variability of fall soil moisture and spring snow water equivalent within a mountainous Sub-Arctic watershed. In: Proceedings of the 60th Eastern Snow Conference, pp. 127–139.

Kershaw, G.P., McCulloch, J., 2007. Midwinter snowpack variation across the Arctic treeline, Churchill, Manitoba, Canada. Arctic Antarctic and Alpine Research 39 (1), 9–15.

Laternser, M., Schneebeli, M., 2003. Long-term snow climate trends of the Swiss Alps (1931–99). International Journal of Climatology 23, 733–750.

Liston, G.E., Sturm, M., 2002. Winter precipitation patterns in arctic Alaska determined from a blowing-snow model and snow-depth observations. Journal of Hydrometeorology 3 (6), 646–659.

Lundberg, A., Richardson–Naslund, C., Andersson, C., 2006. Snow density variations: consequences for ground-penetrating radar. Hydrological Processes 20 (7), 1483–1495.

Magnusson, J., Jonas, T., Lopez-Moreno, J.I., Lehning, M., 2009. Snow cover response to climate change in a high alpine and half glaciated basin in Switzerland. Hydrology Research, accepted for publication.

Marchand, W.D., Killingtveit, A., 2004. Statistical properties of spatial snowcover in mountainous catchments in Norway. Nordic Hydrology 35 (2), 101–117.

Meloysund, V., Leira, B., Hoiseth, K.V., Liso, K.R., 2007. Predicting snow density using meteorological data. Meteorological Applications 14 (4), 413–423.

Mizukami, N., Perica, S., 2008. Spatiotemporal characteristics of snowpack density in the mountainous regions of the Western United States. Journal of Hydrometeorology 9 (6), 1416–1426.

Onuchin, A.A., Burenina, T.A., 1996. Climatic and geographic patterns in snow density dynamics, Northern Eurasia. Arctic and Alpine Research 28 (1), 99–103.

Pomeroy, J.W., Gray, D.M., 1995. Snow Accumulation, Relocation and Management. National Hydrology Research Institute Science Report No. 7, p. 144.

Rohrer, M., Braun, L.N., Lang, H., 1994. Long-term records of snow cover water equivalent in the Swiss Alps: 1. Analysis.. Nordic Hydrology 25, 53–64.

Rovansek, R.J., Kane, D.L., Hinzman, L.D., 1993. Improving estimates of snowpack water equivalent using double sampling. In: In: Proceedings of the 61st Western Snow Conference, pp. 157–163.

Sturm, M., Holmgren, J., 1998. Differences in compaction behaviour of three climate classes of snow. Annals of Glaciology 26, 125–130.

Sturm, M., Holmgren, J., Liston, G.E., 1995. A seasonal snow cover classification system for local to global applications. Journal of Climate 8 (5), 1261–1283.

Sturm, M., Liston, G.E., 2003. The snow cover on lakes of the Arctic Coastal Plain of Alaska, USA. Journal of Glaciology 49 (166), 370–380.

Sturm, M. et al., submitted for publication. Estimating local to global snow water resources using snow depth data and snow climate classes. Journal of Hydrometeorology.

Watson, F.G.R., Anderson, T.N., Newman, W.B., Alexander, S.E., Garrott, R.A., 2006. Optimal sampling schemes for estimating mean snow water equivalents in stratified heterogeneous landscapes. Journal of Hydrology 328 (3–4), 432–452.